

The Structure and Morphology of the Skin of Polyethersulfone Ultrafiltration Membranes: A Comparative Atomic Force Microscope and Scanning Electron Microscope Study

A. K. FRITZSCHE,^{1,*} A. R. AREVALO,¹ A. F. CONNOLLY,¹ M. D. MOORE,¹ V. ELINGS² and C. M. WU²

¹BIOKEN Separations, Inc. (currently CUNO Separations Systems Division), 50 Kerry Place, Norwood, Massachusetts 02062, and ²Digital Instruments, Inc., 6780 Cortona Drive, Santa Barbara, California 93117

SYNOPSIS

Atomic Force Microscopy (AFM) and Scanning Electron Microscopy (SEM) were used to investigate the surface structure and morphology of 10,000, 30,000, and 100,000 dalton molecular weight cutoff (MWCO) polyethersulfone (PES) ultrafiltration membranes, and the results are compared. Although both approaches reveal the pore structure in the 30,000 and 100,000 MWCO membranes, the pore diameters derived from SEM are smaller than those measured by AFM. This discrepancy is a result of the diminution in pore dimensions during the sample preparation for SEM, that is, the solvent exchange procedure needed to remove the water from the membrane prior to the high vacuum gold coating deposition step. In contrast to SEM, which requires a high vacuum both during heavy metal coating and during examination, AFM can be performed on wet ultrafiltration membranes. Consequently, the potential of altering the membranes' pore structures during sample preparation is eliminated. Therefore, the pore diameters obtained from AFM are more accurate than those derived from SEM.

INTRODUCTION

Phase inversion of polymer sols is widely used to prepare integrally skinned membranes for reverse osmosis, microfiltration, ultrafiltration, and gas separations. In these integrally skinned membranes, the skin and substructure are composed of the same material. The skin layer determines both the permeability and selectivity of a gas separation, or reverse osmosis membrane, and the flux and rejection characteristics of an ultrafiltration or microfiltration membrane. In contrast, the porous substructure functions primarily as a physical support for the skin. Therefore, research efforts to correlate the performance of integrally skinned membranes with their structures and morphologies have justifiably focused on the skin layer at which the separation is effected.

The scanning electron microscope (SEM) is a powerful tool with which to investigate the structure of polymeric integrally skinned membranes.¹ However, the utilization of an electron beam under high vacuum to probe the structure of the membrane limits the SEM's effectiveness. Membranes are fabricated from polymeric materials, which possess low conductivity, and, therefore, bombarding the sample with electrons can lead to charging unless the sample is coated with a heavy metal, such as gold, platinum, or palladium. However, the coating process itself may be destructive and obscures finer details. For example, grain sizes of 5–10 nm have been reported in Au/Pd replicas.² Another problem in the study of organic films, such as those constituting the skin of an asymmetric membrane, is beam induced damage. In fact, the assemblies of nodule aggregates constituting the outer surface of gas separation membranes have been shown to separate upon exposure to an electron beam.² Equivalent or worse beam induced damage may be expected in ultrafiltration/microfiltration membranes because lower

* To whom correspondence should be addressed.

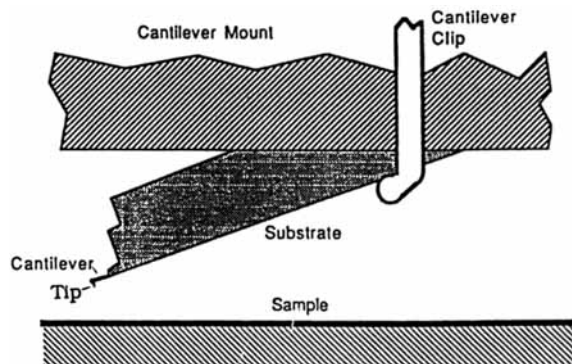


Figure 1 Scheme for an atomic force microscope showing the tip fastened to a cantilever spring that has a spring constant lower than the effective spring between two atoms.

concentrations of polymer in the sol are used in their preparation.

In addition, ultrafiltration and microfiltration membranes effect their separations by virtue of pores, which exist in their skin layers. Unless proper drying techniques are employed, such as solvent exchange, collapse of the pore structure may result,

and employment of such techniques does not insure the absence of alteration of the fine pore structure. Consequently, the structure of an ultrafiltration or microfiltration membrane, as revealed by scanning electron microscopy, may not be identical to that which existed prior to its conversion into a specimen suitable for SEM examination. Therefore, a greater understanding of the surface structure of the skin layer of an asymmetric membrane might be gained if the structure could be examined without drying, without coating, and without the application of a high energy electron beam.

Atomic force microscopy (AFM) circumvents the limitations of scanning electron microscopy. AFM operates as an ultra-low-force imaging surface profiler.³ An extremely sharp tip, attached to a microcantilever arm, is brought into contact with a sample as shown in Figure 1. A laser beam is reflected from the cantilever to an optical position sensor, as illustrated in Figure 2. The beam is subsequently converted into a displayed image while the tip is scanned over the surface. Therefore, the three dimensional features on the sample are tracked and recorded.⁴ In order to avoid damage to an array of organic molecules, the interaction force must be kept

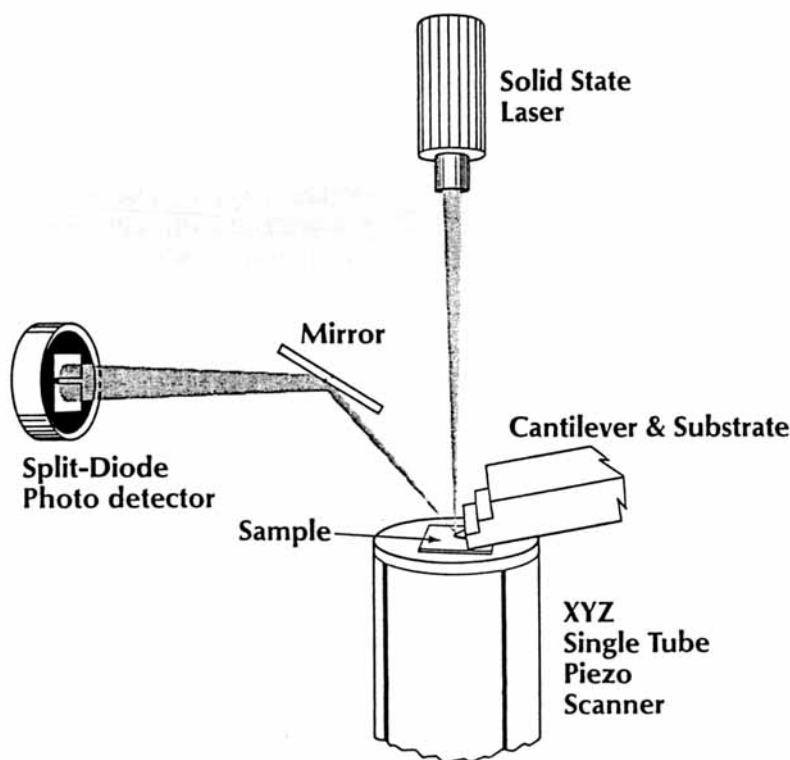
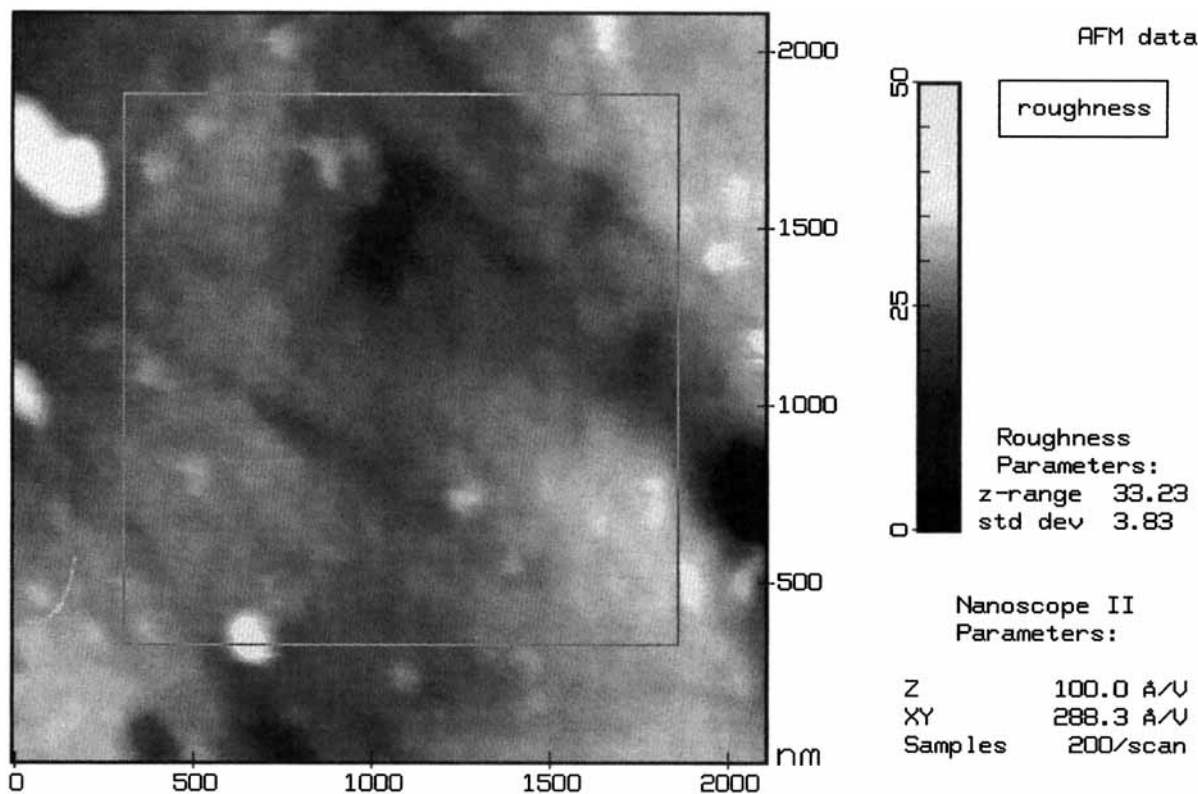


Figure 2 Drawing of an AFM that utilizes an optical lever technique for sensing cantilever deflection.



BIOKEN MEMBRANE SAMPLE B
Data taken Mon Feb 04 13:21:34 1991
Buffer 1(BK-B1), Rotated 0°, XY axes [nm], Z axis [nm]

Figure 3 A top view image of a 10K MWCO polyethersulfone ultrafiltration membrane surface, taken with an Atomic Force Microscope with bar at right indicating the vertical deviation.

below 10^{-8} N, which can be achieved if the sample, tip, and cantilever are immersed in a liquid, such as water or ethanol.⁵ Consequently, AFM has successfully imaged surfaces with absorbed organic molecules, such as sorbic acid, DNA, and proteins.⁶ In fact, the use of smaller interaction forces and operation in water have permitted the observation of biological samples in physiologically relevant environments, such as the imaging in real time of the polymerization of fibrin.⁶

The ability of AFM to image with low interaction forces and in an aqueous environment suggests that AFM could also provide useful information on the surface layer of asymmetric, integrally-skinned membranes for ultrafiltration. Therefore, it is the purpose of this article to report the results of an AFM examination of polyethersulfone ultrafiltration membranes and to compare them with those obtained by SEM.

EXPERIMENTAL

Polyethersulfone ultrafiltration membranes with 10,000, 30,000, and 100,000 dalton molecular weight cutoffs were selected for this study. The molecular weight cutoffs for these ultrafiltration membranes were determined by challenging the membrane with proteins of known molecular weights. The molecular weight at which the membrane exhibits at least a 90% rejection of the protein to passage defines its molecular weight cutoff. These membranes are commercially available from BIOKEN Separations and are fabricated from proprietary formulations cast on a nonwoven polyolefin fabric substrate. The 10,000 MWCO formulation was developed by a team, directed by the late B. Sachs, while the 30,000 and 100,000 formulations have been developed by the BIOKEN authors of this article. The performances (pure water flux, water flux with dissolved protein,

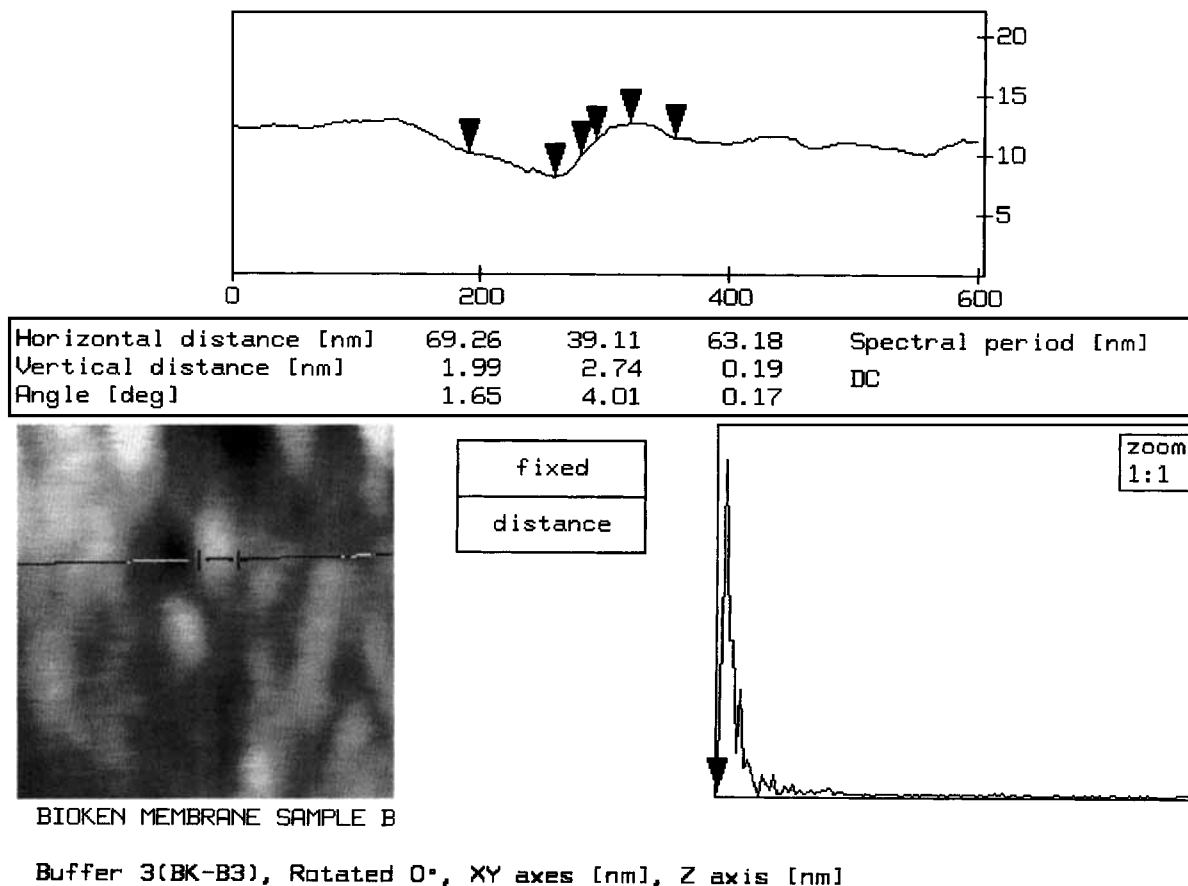


Figure 4 A vertical displacement profile of a 10K MWCO polyethersulfone ultrafiltration membrane surface, taken from horizontal line across insert image by AFM.

and percent protein rejections) were obtained using 44 mm diameter membrane disks in Amicon 8050, magnetically-stirred ultrafiltration cells at room temperature and 55 psig. Each membrane sample was tested in triplicate.

The proteins used to challenge the membranes were purchased from Sigma Chemical Company, St. Louis, Missouri, USA. The concentrations of proteins in the permeate and retentate solutions were determined from their absorbances using a Perkin-Elmer Lambda 3A UV/visible spectrophotometer. The wavelengths at which the absorbances were measured were 360 nm for vitamin B-12, 409 nm for myoglobin, 280 nm for ovalbumin, 278 nm for bovine albumin, and 278 nm for gamma-globulin. These proteins had the following molecular weights: vitamin B-12, 1400; myoglobin, 17,500; ovalbumin, 44,000; bovine albumin, 66,000; and gamma-globulin, 150,000. The performance data used to characterize the membranes were obtained using wet membranes, which had been stored in 18 Mohm-cm water under refrigeration prior to testing. Sam-

ples for evaluation by AFM were placed in polyethylene bags with 18 Mohm-cm, ultrapure water to maintain their moisture levels. The polyethylene bags were then heat sealed and were subsequently shipped to Digital Instruments, Inc., Santa Barbara, California, USA, for examination using the NanoScope AFM.

In contrast to the samples for AFM, the samples for SEM were dried by a solvent exchange process, which is routinely used in this laboratory to prepare PES ultrafiltration membranes for SEM analysis. The wet ultrafiltration membrane samples were first immersed for five minutes in isopropanol to remove the water from the membrane. Subsequently, the samples were placed in hexane for 1 h. Hexane then exchanged with isopropanol. Finally, these membranes were allowed to dry in the air. The dried membranes were also placed in polyethylene bags, which were subsequently heat sealed. These samples were sent to AT&T Analytical Services, Allentown, Pennsylvania, USA, for analysis on the Hitachi S-800 scanning electron microscope with an attainable

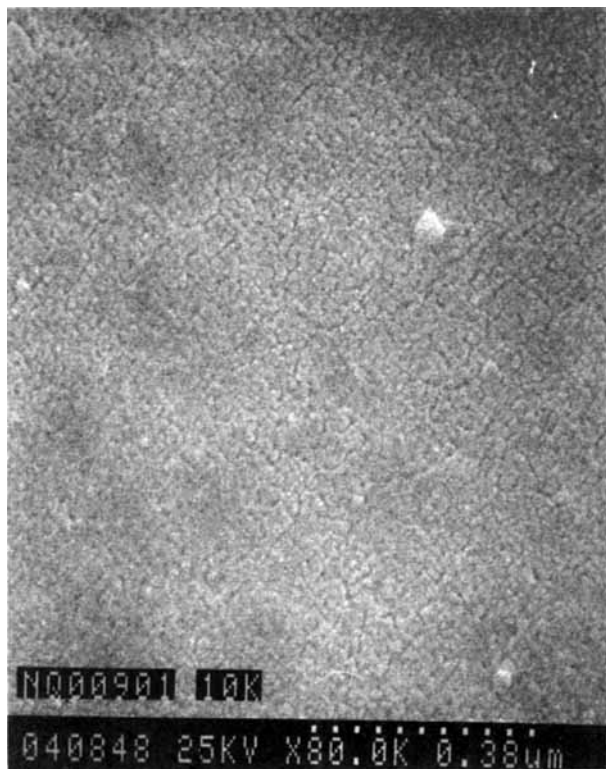


Figure 5 A SEM photomicrograph of a 10K MWCO polyethersulfone ultrafiltration membrane surface at 80K magnification.

resolution of 2 nm. However, the resolution at the time of the analysis was reported to be between 3 and 5 nm. The samples were prepared by fracture after freezing in liquid nitrogen; then they were Au coated to eliminate charging. The smooth upper surface of each sample was examined at 0° tilt and at 80,000 magnification. Also, the outer edges of the cross-sections nearest the upper smooth surfaces of the samples were photographed at 80,000X. Eleven dots in a row can be observed in the lower right hand corner of each SEM photomicrograph. These dots indicate the scale of the photomicrograph with 38 nm between each two adjacent dots, so that the entire assembly represents 380 nm.

Forty-four mm membrane disks, which had been dried by solvent exchange, that is, the first 5 min in isopropanol followed by 1 h in hexane prior to drying in air, were rendered suitable for water flux and protein rejection characterization by reversing the solvent exchange process. Therefore, dried membranes were soaked in hexane for 1 h prior to a 5 min immersion in isopropanol, and finally they were placed in 18 Mohm-cm water until characterized in the Amicon 8050 magnetically-stirred ultrafiltration

cells. The performance characteristics of these samples were also measured in triplicate for comparison with the original values.

RESULTS AND DISCUSSION

10K MWCO Polyethersulfone Ultrafiltration Membrane

The structure of the surface of the 10K MWCO PES membrane, as revealed by the atomic force microscope, is shown in Figures 3 and 4. Figure 3 is a topview image of the surface, showing an area slightly greater than 2000 nm × 2000 nm. The bar at the right side of the image indicates the vertical deviations in the sample with the white regions being the highest points and the dark regions being the depressions. The vertical range, reflected by the bar to the right of the image, is 33.2 ± 3.8 nm. Several dark regions, reminiscent of pores, can be seen in this image. However, measurements of the vertical deviations along the horizontal line, seen in the insert in the lower left corner of Figure 4, cannot differentiate whether these structures are pores or depressions in the membrane's irregular surface. In fact, little detail of the fine structure of the surface of the 10K MWCO membrane can be discerned. The distance variations along this profile are shown in the upper portion of Figure 4 by three pairs of cursors. The vertical and horizontal distances between each pair of cursors are given. In Figure 4, for example, the first and second, third and fifth, and fourth and sixth cursors are these three pairs when counting from left-to-right. On the AFM screen, each pair is a different color. Consequently, the first

Table I Performance of 10K MWCO Polyethersulfone Ultrafiltration Membrane Before and After Solvent Exchange Cycle

	Before	After ^a
Water Flux (LMH) ^b	843 ± 75	0
Water Flux with Vitamin B-12 (LMH) ^b	520 ± 99	—
% Rejection Vitamin B-12	12.9 ± 2.5	—
Water Flux with Myoglobin (LMH) ^b	127 ± 10	—
% Rejection Myoglobin	99.9 ± .05	—

^a Membrane + water, then membrane + isopropanol, then membrane + hexane, then membrane + air, then membrane + hexane, then membrane + isopropanol, and membrane + water.

^b LMH, liters per square meter per h.

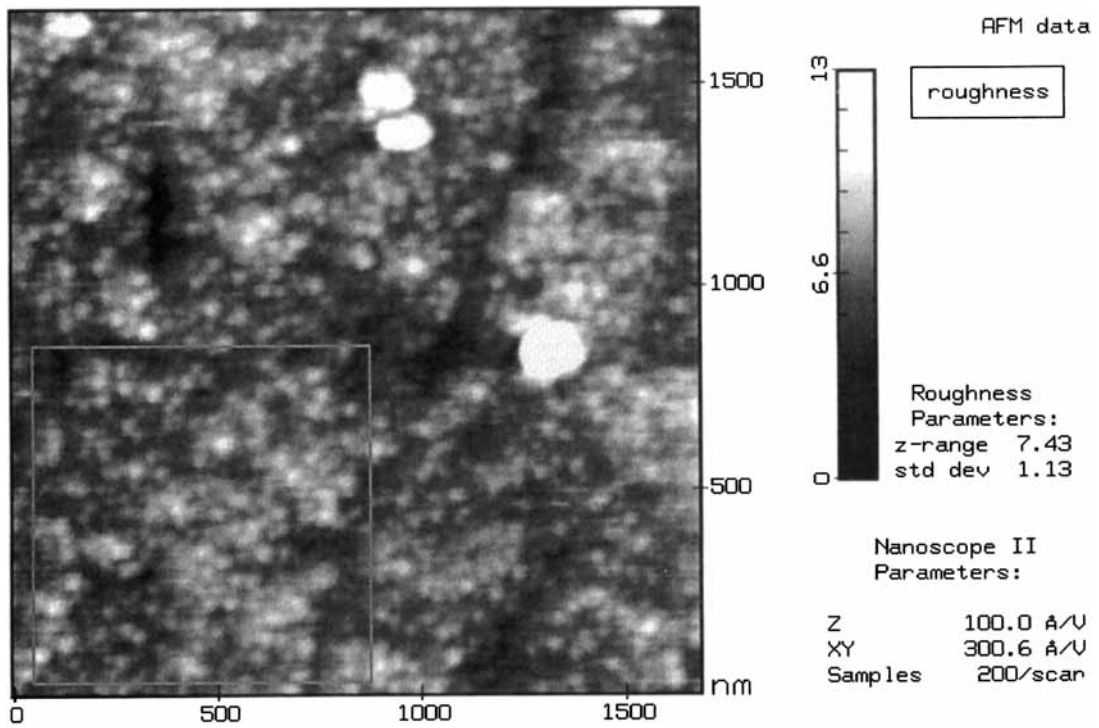


Figure 6 A topview image of a 30K MWCO polyethersulfone ultrafiltration membrane surface by AFM, covering the area 1500 nm × 1500 nm.

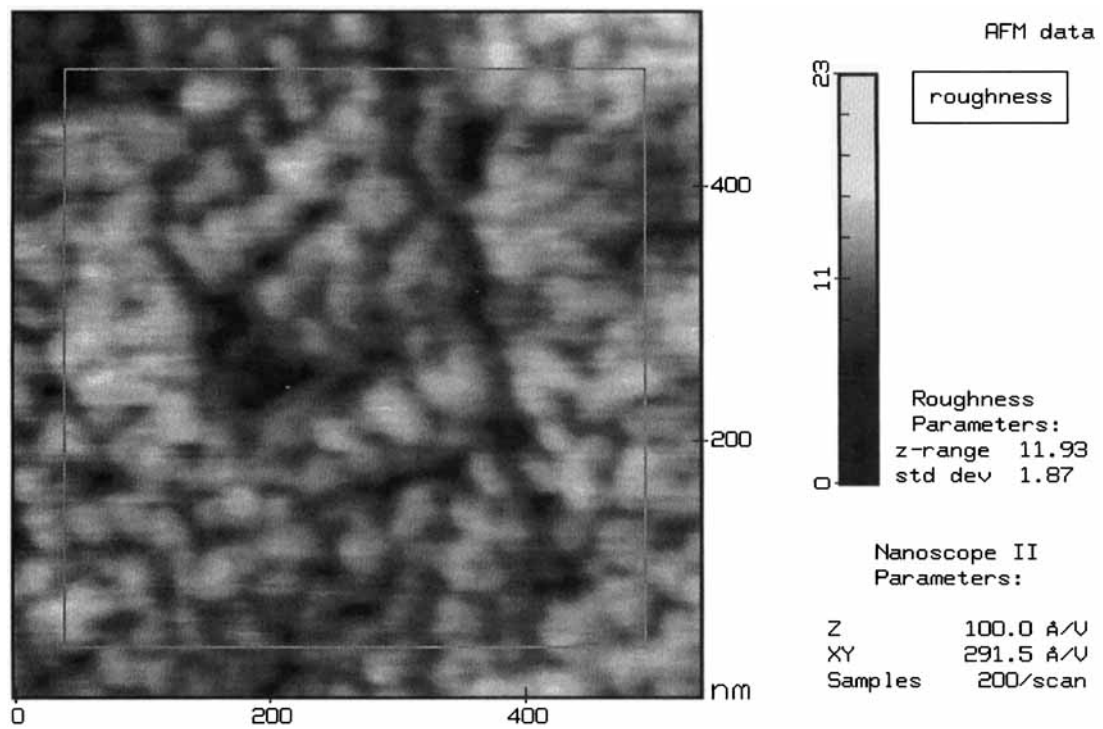
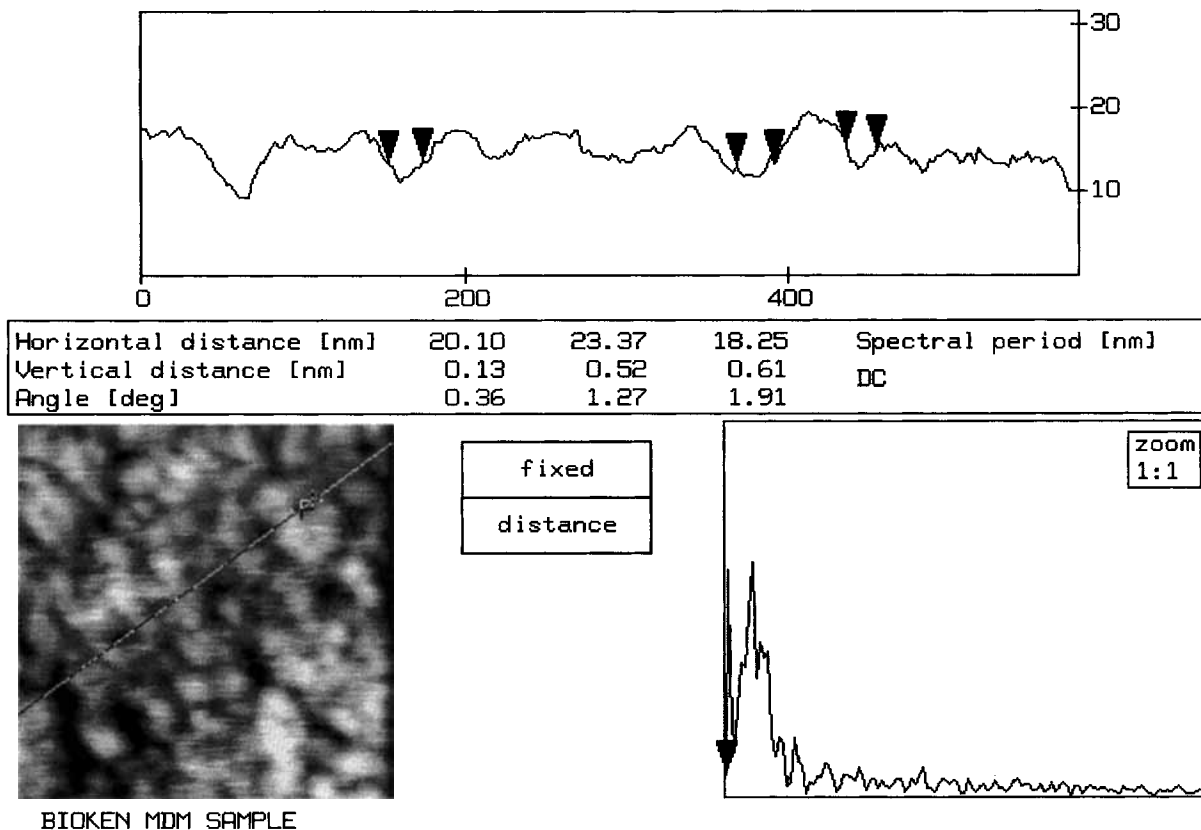


Figure 7 A topview image of a 30K MWCO polyethersulfone ultrafiltration membrane surface by AFM, covering the area 500 nm × 500 nm.



Buffer 2(MDM15), Rotated 0°, XY axes [nm], Z axis [nm]

Figure 8 A vertical displacement profile of a 30K MWCO polyethersulfone ultrafiltration membrane surface, taken from diagonal line across insert image by AFM.

pair represents a horizontal distance of 69.26 nm and a vertical distance of 1.99 nm, the second pair of 39.11 nm and 2.74 nm, and the third pair of 63.18 nm and 0.19 nm, respectively. The depth displacement along the profile results from the depth to which the AFM tip can fit into a depression or pore, and, in the 10K MWCO PES ultrafiltration membrane, the pores are too small to be resolved by this technique. The graph in the lower right corner of Figure 4 is a Fourier transform of the height profile with the power spectrum (ordinate) graphed against the spatial frequency (abscissa).

A scanning electron micrograph of the upper surface of the 10K PES membrane is shown in Figure 5. Examination reveals a dense, tightly packed, grainy structure, reminiscent of that resulting from assemblies of nodule aggregates^{2,7-11} or grains of the coating material. As with the AFM, the pores are difficult to discern because the 3-5 nm pore size needed to reject 10,000 dalton proteins is equivalent to the limits of resolution of the Hitachi S-800 SEM.

Therefore, it cannot be determined by inspection of the SEM photomicrograph whether pores exist in the interstitial regions between adjacent nodule aggregates or whether these regions are simply depressions in a continuous surface. Water flux measurements and protein challenge tests on 10K MWCO PES ultrafiltration membranes, which were dried and then rewet by solvent exchange, indicate that the surface of the membrane examined by SEM is continuous. As shown in Table I, no water could be transported across the solvent exchanged PES ultrafiltration membrane at 55 psi differential pressure. In contrast to these results, the PES ultrafiltration membrane, which remains wet, exhibits a high water flux, low vitamin B-12 rejection, and high myoglobin rejection.

Consequently, the pores existing in a 10K MWCO PES ultrafiltration membrane are too small to be resolved by AFM and too small for the solvent exchange procedure to prepare them for examination by SEM without closure of the pores.

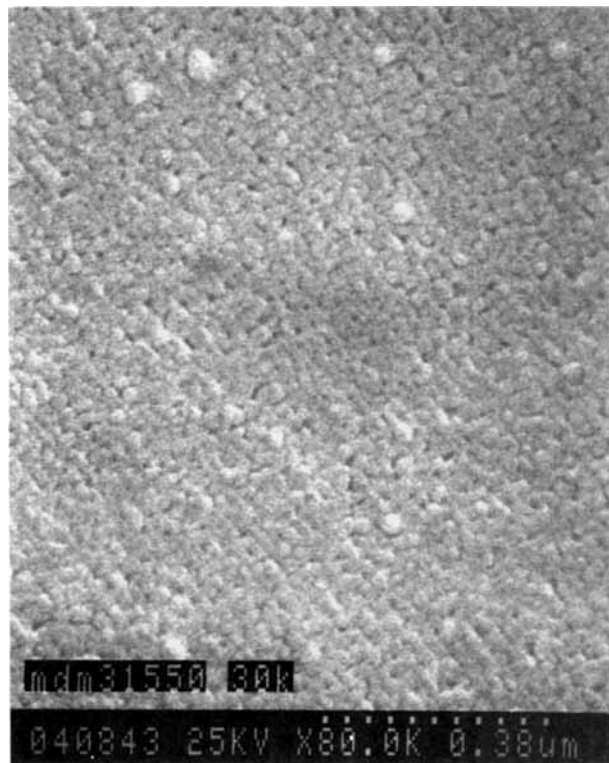


Figure 9 A SEM photomicrograph of a 30K MWCO polyethersulfone ultrafiltration membrane surface at 80K magnification.

30K MWCO Polyethersulfone Ultrafiltration Membrane

The structure of the surface of the 30K MWCO PES ultrafiltration membrane, as revealed by AFM, is shown in Figures 6–8. Figures 6 and 7 are both topview images, differing only in their xy scales. Figure 6 shows an area approximately 1500 nm × 1500 nm. Unlike Figure 3, which shows the surface of the 10K MWCO PES membrane, a grainy structure reminiscent of nodule aggregations can be seen. These aggregations are the lighter regions. Darker regions exist where adjacent aggregations come into contact. Also, very dark regions, indicative of pores, can be seen. The vertical range, reflected by the bar to the right of the image, is 7.43 ± 1.13 nm. The fine structure of the surface, resulting from the nodule aggregations, their interstitial depressions, and an occasional pore, is seen in Figure 7, which shows an area approximately 500 nm × 500 nm. The vertical range can be expanded independently of the xy plane. Therefore, the vertical range in Figure 7, indicated by its bar, is 11.93 ± 1.87 nm. The measurements along the diagonal line, seen in the insert at the lower left of Figure 8, indicate that the pores

are 15 nm to 25 nm in diameter. The distances between each pair of cursors as one proceeds from left to right in the profile at the top of Figure 8 is 20.10 nm, 23.37 nm, and 18.25 nm. Pores, 15–25 nm in diameter, are exactly within the size range that would retard passage of 30,000 molecular weight polysaccharides.¹² The tip of the AFM could only penetrate 4 nm to 6 nm into pores with this range of diameters.

A scanning electron micrograph of the upper surface of the 30K MWCO PES membrane is given in Figure 9. The pores in its surface can be seen, and measurements taken from this photomicrograph suggest that the average pore diameter is 13.2 ± 3.6 nm, which is less than that obtained by AFM. This diminution of the pore size is a result of the solvent exchange procedure utilized to prepare the PES ultrafiltration membranes for SEM analysis. The degree of this alteration may be inferred from water flux measurements and protein challenge tests on 30K MWCO ultrafiltration membranes, which were dried by solvent exchange and then rewet by reversing the solvent exchange procedure. The results, given in Table II, show not only a 70% decline in pure water flux, but an almost fifty-fold increase in myoglobin rejection over the rejection of the untreated membrane. Such rejections imply that the pore size in the solvent-exchanged membrane is in the 8 nm to 10 nm range.

100K MWCO Polyethersulfone Ultrafiltration Membrane

The structure of the surface of the 100K MWCO PES ultrafiltration membrane, as revealed by AFM,

Table II Performane of 30K MWCO Polyethersulfone Ultrafiltration Membrane Before and After Solvent Exchange Cycle

	Before	After ^a
Water Flux (LMH) ^b	1450 ± 60	476 ± 41
Water Flux with Myoglobin (LMH) ^b	413 ± 12	44 ± 6
% Rejection Myoglobin	1.7 ± .7	82.4 ± 2.2
Water Flux with Ovalbumin (LMH) ^b	170 ± 12	79 ± 3
% Rejection Ovalbumin	94.0 ± .4	94.1 ± .3

^a Membrane + water, then membrane + isopropanol, then membrane + hexane, then membrane + air, then membrane + hexane, then membrane + isopropanol, and finally membrane + water.

^b LMH, liters per square meter per h.

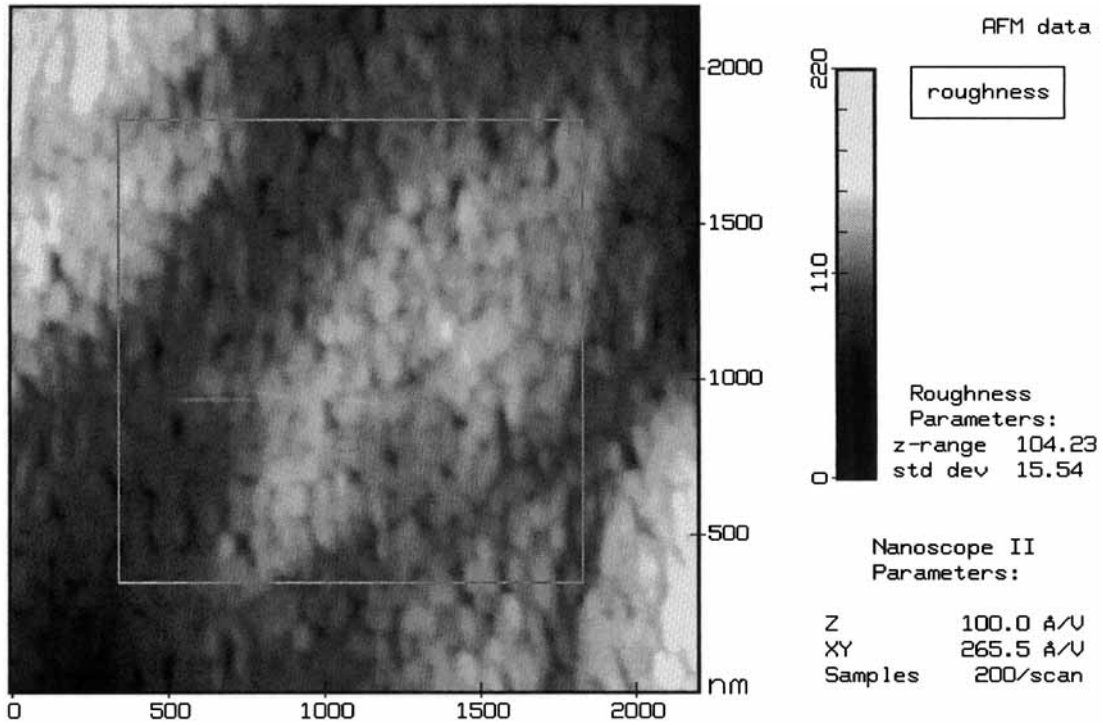


Figure 10 A topview image of a 100K MWCO polyethersulfone ultrafiltration membrane surface by AFM, covering the area 2000 nm × 2000 nm.

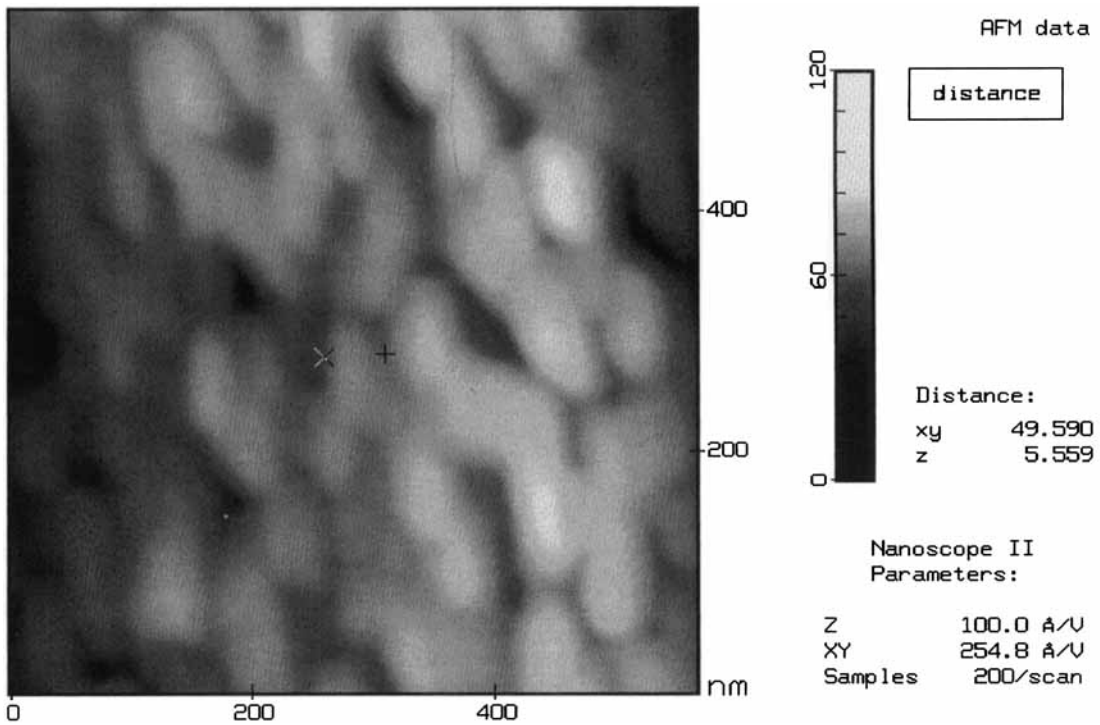


Figure 11 A topview image of a 100K MWCO polyethersulfone ultrafiltration membrane surface by AFM, covering the area 600 nm × 600 nm.

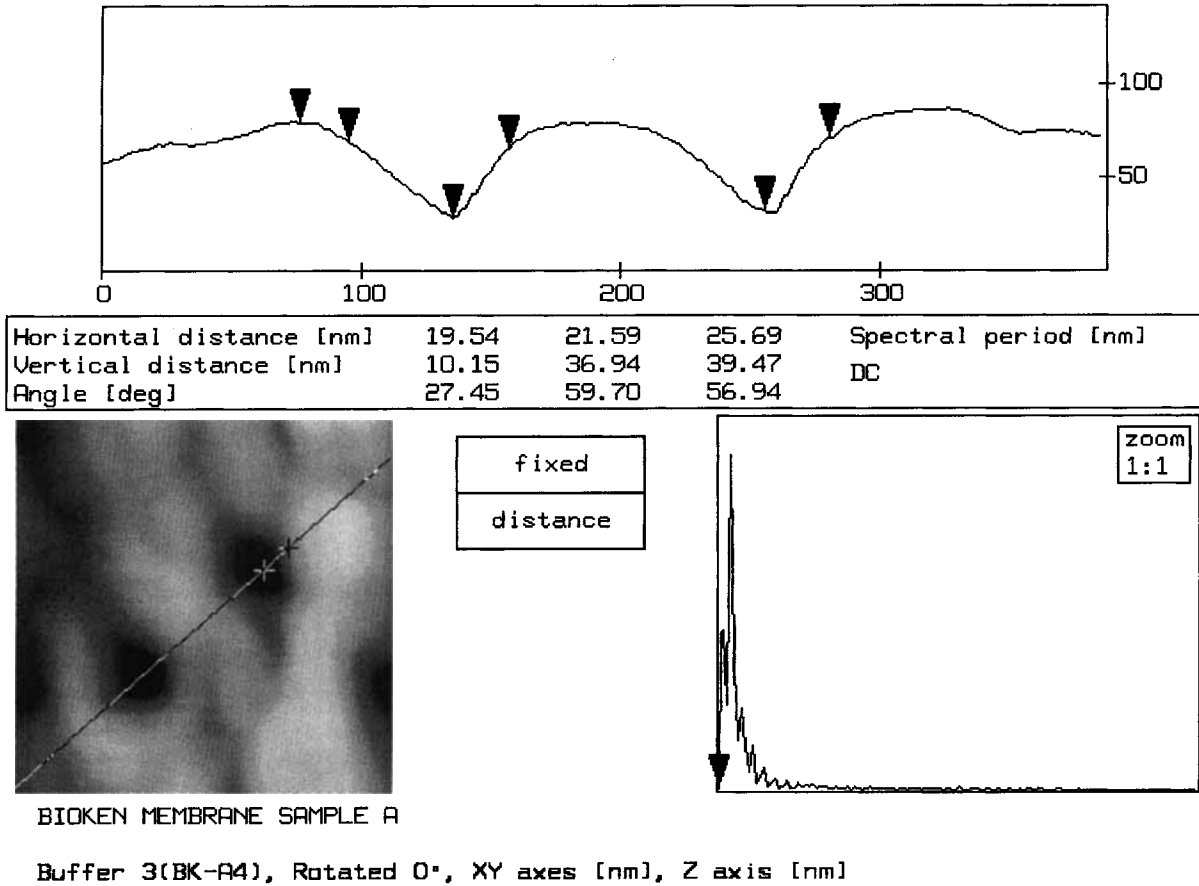


Figure 12 A vertical displacement profile of a 100K MWCO polyethersulfone ultrafiltration membrane surface, taken from diagonal line across insert image by AFM.

is shown in Figures 10–12. Figures 10 and 11 are both topview images. They differ both in their xy scales, with Figure 10 showing an area slightly greater than 2000 nm × 2000 nm, and with Figure 11 being a 600 nm × 600 nm image, and in their roughness scales of the bars, with that in Figure 10 representing a vertical range of 104.23 ± 15.54 nm and that in Figure 11 representing a vertical range of 49.95 ± 5.56 nm. In both, dark regions, which are believed to be pores, can be seen. Measurements of the vertical deviations along the diagonal line, seen in the insert in the lower left hand of Figure 12, indicate that the pores are 50–60 nm in diameter, which is the pore diameter range in the Filtration Spectrum equivalent to a 100,000 molecular weight polysaccharide.¹² The measurements also indicate that the pores are also about 50 nm in depth. However, this measurement just reflects how far the AFM tip could fit into the pores. Examination of Figures 10–12 indicates that the surface of the 100K MWCO PES ultrafiltration membrane is rougher than the surfaces of the 10K MWCO and 30K MWCO PES

ultrafiltration membranes. It is suspected that this increase in surface roughness arises from several factors. First, the AFM tip can penetrate deeper into the larger diameter pores of the 100K MWCO membrane than it can in those pores of the 30K MWCO membrane; the tip is too large to penetrate into the pores of the 10K MWCO membrane. Second, the 30K MWCO and 100K MWCO PES ultrafiltration membranes are fabricated using a formulation that accelerates the phase inversion process over that used to produce the 10K MWCO PES membrane, and the 100K MWCO PES ultrafiltration membrane is so fabricated that its process conditions further accelerate its rate of coagulation over those used to produce the 30K MWCO PES ultrafiltration membrane. It has been shown that acceleration of the kinetics of the phase inversion process yields skins composed of less tightly packed arrays of nodule aggregates.^{2,13,14} Consequently, these nodule aggregates suffer less distortion during skin formation and, therefore, are more readily discernible. The presence of less tightly packed, less deformed nodule aggre-

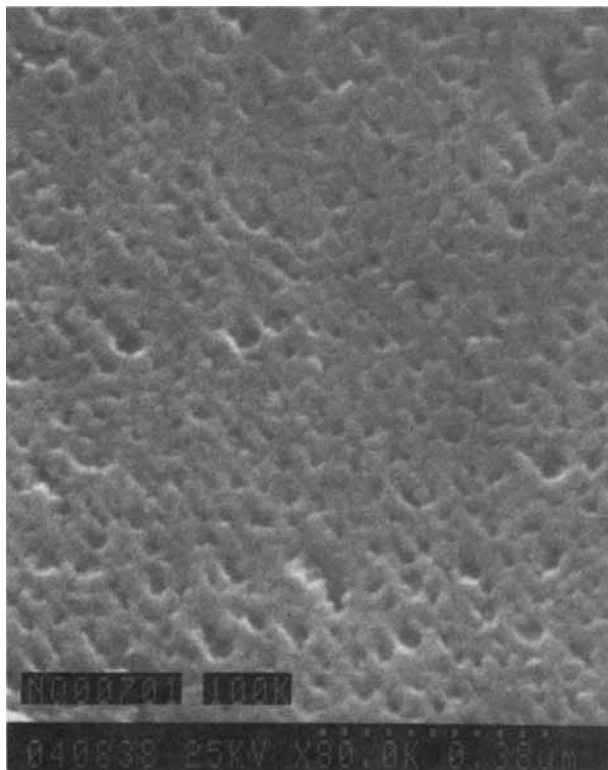


Figure 13 A SEM photomicrograph at a 100K MWCO polyethersulfone ultrafiltration membrane surface at 80K magnification.

gates in the skin would also contribute to a higher degree of roughness in its surface.

A scanning electron micrograph of the upper surface of the 100K PES membrane is shown in Figure 13. The pores are readily seen. However, measurements obtained from the SEM photomicrographs suggest that the average diameter of these pores is 22 ± 9 nm, which is less than half the value obtained from the AFM measurement. The water flux measurements and protein challenge tests on 100K MWCO PES ultrafiltration membranes, which were dried and then rewet by solvent exchange, also indicate that the pore sizes were altered by the preparation of samples for the SEM, as shown in Table III. Although the performance changes resulting from the solvent exchange technique are not so great as those observed with the 30K MWCO PES ultrafiltration membranes similarly treated, the pure water flux declined about 20% with larger percentage declines in water fluxes with challenge proteins present in the rejection tests. Also, little change was observed in the percent rejections of the challenge proteins. The results suggest that the smallest pores are closed during the solvent exchange process, the

intermediate sized pores diminished, and the largest pores remain relatively unaffected. So, the structures identified as pores in the SEM photomicrographs of these PES ultrafiltration membranes are not identical to those existing in these membranes prior to preparation for SEM analysis by solvent exchange. However, without the solvent exchange pretreatment, the alteration of the surface structure of the 100K MWCO PES membrane would have been even more dramatic. 100K MWCO PES membranes were dried overnight in air. They were then rewet by exposing the membranes in turn to hexane and isopropanol, prior to the water flux test. These membranes exhibited water fluxes of 980 ± 50 LMH, or a 62% decline from the original water flux value.

CONCLUSIONS

Both Atomic Force Microscopy and Scanning Electron Microscopy can be used to detect and to measure pores in ultrafiltration membranes rated at a 30,000 molecular weight cutoff or greater. Neither technique could resolve the surface pore structure in 10,000 MWCO membranes. So, the limit of resolution for these two techniques resides within these two boundaries.

However, the procedures necessary to prepare polyethersulfone ultrafiltration membranes for SEM examination, solvent exchange drying, and heavy metal coating in high vacuum, alter the surface pore structure or obscure the ultrafine structure. Consequently, the porosity, as reflected by SEM photomicrographs, is not identical to that of the virgin membrane. In contrast, AFM can be used with the virgin membrane. The membrane, in fact, is im-

Table III Performance of 100K MWCO Polyethersulfone Ultrafiltration Membrane Before and After Solvent Exchange Cycle

	Before	After ^a
Water Flux (LMH) ^b	2550 \pm 240	2060 \pm 290
Water Flux with Bovine Albumin (LMH) ^b	1120 \pm 90	590 \pm 170
% Rejection Bovine Albumin	10.2 \pm 5.8	2.1 \pm 2
Water Flux with gamma-globulin (LMH) ^b	87 \pm 4	66 \pm 1
% Rejection gamma-globulin	98.3 \pm .3	97.3 \pm .2

^a Wet membrane, then isopropanol exchange, then hexane exchange, then air dry, then hexane, then isopropanol, and finally water.

^b LMH, liters per square meter per h.

mersed in a liquid, such as water, as its surface is being probed. The resultant AFM micrographs with the accompanying vertical profile measurements yield values for pore diameters at the skin surface that are not only larger than those determined from SEM, but coincide with the diameters predicted from protein and polysaccharide challenge tests. Consequently, Atomic Force Microscopy yields realistic measurements of pore diameters at the surface of ultrafiltration membranes, whose surface structures are altered by solvent exchange preparatory techniques for SEM. Based on these results, it is predicted that AFM will become an increasingly-used instrument to study ultrafiltration membranes, and will complement SEM.

The authors wish to express their gratitude to S. Antoniazzi for typing the manuscript and to H. Polishook for his assistance.

REFERENCES

1. R. E. Kesting, *Synthetic Polymeric Membranes, A Structural Perspective, 2nd Ed.*, Wiley, New York, 1985.
2. A. K. Fritzsche, B. L. Armbruster, P. B. Fraundorf, and C. J. Pellegrin, *J. Appl. Polym. Sci.*, **39**, 1915 (1990).
3. G. Binnig, C. F. Quate, and C. Gerber, *Phys. Rev. Lett.*, **56**, 930 (1986).
4. D. Rugar and P. Hansma, *Physics Today*, **23**, October 1990.
5. O. Marti, B. Drake, P. K. Hansma, *Appl. Phys. Lett.*, **51**, 484 (1987).
6. B. Drake, C. B. Prater, A. L. Weisenhorn, S. A. Gould, T. R. Albrecht, C. F. Quate, D. S. Cannell, H. G. Hansma, and P. K. Hansma, *Science*, **243**, 1586 (1989).
7. R. Schultz and S. Asunmaa, *Rec. Prog. Surface Sci.*, **3**, 291 (1970).
8. R. Kesting, *J. Appl. Polym. Sci.*, **17**, 1771 (1973).
9. R. Kesting, U.S. Pat. 3,884,801 (1975).
10. K. Kamide and S. Manabe, in *Material Science of Synthetic Membranes*, D. Lloyd, Ed., American Chemical Society Symposium Series, 269, American Chemical Society, Washington, DC, 1985.
11. M. Panar, H. Hoehn, and R. Herbert, *Macromolecules*, **6**, 777 (1973).
12. *The Filtration Spectrum*, Osmonics, Inc., FS-8409 P/N17978.
13. A. K. Fritzsche, C. A. Cruse, R. E. Kesting, and M. K. Murphy, *J. Appl. Polym. Sci.*, **41**, 713 (1990).
14. A. K. Fritzsche, C. A. Cruse, M. K. Murphy, and R. E. Kesting, *J. Memb. Sci.*, **54**, 29 (1990).

Received May 29, 1991

Accepted October 21, 1991